Electronic Supplementary Material (ESI) for Journal of Materials Chemistry A.


# Supplementary materials

## Facile synthesis of tin-doped polymeric carbon nitride with a hole-trapping center for efficient charge separation and photocatalytic hydrogen evolution

Zhiwei Liang,[a] Yuguo Xia,[a] Guiming Ba,[a] Haiping Li,*[a] Quanhua Deng [b] and Wanguo Hou [b]

[a] *National Engineering Research Center for Colloidal Materials, Shandong University, Jinan 250100, P. R. China;*
[b] *Key Laboratory for Colloid and Interface Chemistry (Ministry of Education), Shandong University, Jinan 250100, P. R. China.*

*Email: hpli@sdu.edu.cn

## S1. Experimental section

### *S1.1. Materials*

Ammonium hexachlorostannate ($(NH_4)_2SnCl_6$, 99.999%) was purchased from Maclin (China). Urea (99.0%), urea-$^{15}N$ (98.5%) with $^{15}N$ abundance of 10%, rhodamine B (RhB, 99.0%), chloroplatinic acid hexahydrate (99.95%), and triethanolamine (99.5%) were bought from Aladdin (China). Poly(3,4-ethylenedioxythiophene)-poly(styrenesulfonate) (PEDOT-PSS, 1.3 wt% in $H_2O$) was purchased from Sigma. All the chemicals were used as received.

### *S1.2. Preparation of Sn-doped CN*

Ten grams of urea and 20, 40, or 60 mg of $(NH_4)_2SnCl_6$ were dissolved in the mixed solution containing 5 mL of $H_2O$ and 25 mL of ethanol, after which the aqueous solution was evaporated at 80 °C under stirring until completely dried. Afterwards, the solid was dried at 60 °C for 24 h in an oven, and put in a crucible with a lid and heated at 550 °C for 4h in $N_2$ with a temperature ramp of 5 °C/min in a tube furnace (OTF-1200X, Hefei Ke Jing Materials Technology Co., LTD., China). After cooling naturally to the room temperature, the sample was dispersed in 100 mL of $H_2O$ and stirred for 24 h. The final product was obtained after filtration, washing with water and dried at 60 °C for 24 h. The product consuming 20, 40, or 60 mg of $(NH_4)_2SnCl_6$ is denoted as CNSn-2, CNSn, and CNSn-6, respectively. Pure CN was prepared by direct calcination of urea via a similar procedure as CNSn. For $^{15}N$ nuclear magnetic resonance (NMR) spectroscopy tests, homogeneously mixed urea-$^{15}N$ and urea with a mass ratio of 1 were used as raw material.

### *S1.3. Characterizations*

Powder X-ray diffraction (XRD) patterns were measured on a PAN analytical X'Pert$^3$ diffractometer with Cu K$\alpha$ radiation ($\lambda$ = 1.54056 Å) and accelerating voltage and current of 40 kV and 40 mA, respectively. X-ray photoelectron spectroscopy (XPS) tests were carried out on a Thermo Scientific Escalab 250Xi spectrometer (UK) with Al K$\alpha$ radiation. Peak positions were calibrated by the C 1s peak at 284.6 eV. Morphologies of samples were observed on a Zeiss Supra55 field emission-scanning electron microscope (SEM, Germany) and a Jeol JEM-2100F transmission electron microscope (TEM, Japan). UV-vis diffuse reflectance spectroscopy was performed on a UH-4150 spectrophotometer (Hitachi, Japan). Photoluminescence (PL) spectra were measured using a Hitachi F-7000 spectrophotometer (Japan) at an excitation wavelength of 400 nm, and excitation and emission slit widths of 5 nm, respectively. Time-resolved fluorescence decay spectra were recorded on an FLS920 time-resolved spectrofluorometer (Edinburgh Analytical Instruments, UK), with excitation and monitoring wavelength of 375 and 460 nm, respectively. $N_2$ sorption isotherms were measured on a Micromeritics TriStar II 3020 instrument (USA) at liquid nitrogen temperature. Samples were degassed at 150 °C for 3 h under vacuum before measurement. Solid-state $^{13}C$ NMR spectrometry tests were carried out on a Bruker AVANCE III 600 spectrometer with DSS as the reference substance. Solid-state $^{15}N$ NMR spectra were measured on a Bruker AVANCE III 400 WB spectrometer with $\alpha$-glycine as the reference substance. Fourier transform infrared (FT-IR) spectra were tested on a Bruker Tensor 27 spectrophotometer.

### *S1.4. Photoelectrochemical tests*

All of photoelectrochemical tests were carried out on a CHI660E electrochemical work station (Chenhua, China) with a standard three-electrode system soaked in a 0.2 M $Na_2SO_4$ solution. Ag/AgCl and Pt wire were used as reference and counter electrodes, respectively. Working electrodes were prepared by coating sample slurries onto clean ITO glass, followed by dried at 60 °C for 24 h and calcined at 200 °C for 2 h in $N_2$ atmosphere. The slurries were obtained by grinding mixtures of 0.01 g of samples, 40 $\mu$L of PEDOT-PSS and 400 $\mu$L of $H_2O$. For photocurrent density and electrochemical impedance spectroscopy (EIS) tests, the applied bias is 0.5 V. A 300-W Xe lamp (CEL-HXF300, Ceaulight, China) with a cutoff filter ($\lambda \geq 420$ nm, CEL-UVIRCUT420, Ceaulight, China) were used as the light source. The EIS tests in the dark and under light irradiation were performed in a frequency range of 0.01 to $10^5$ Hz with an AC voltage amplitude of 5 mV. For Mott-Schottky plot tests, selected frequencies are 0.9 and 1.0 kHz, and 800 $\mu$L of ethanol and 200 $\mu$L of ethylene glycol were substituted for PEDOT-PSS and $H_2O$ for slurry preparation. In addition, the 0.1 M KCl

electrolyte containing 2.5 mM $K_3Fe(CN)_6$ and 2.5 mM $K_4Fe(CN)_6$ was substituted for the 0.2 M $Na_2SO_4$ electrolyte for Mott-Schottky and electrochemical impedance tests.

***S1.5. Photocatalytic performance measurement***

For each photocatalytic hydrogen evolution (PHE) experiment, 20 mg of the sample was dispersed in 80 ml of aqueous solution containing 10 vol% of triethanolamine (TEOA). After sonication for 10 min, the solution was transferred to a reaction cell with 1595 $\mu$L of $H_2PtCl_6$ solution (1 g $L^{-1}$) dropped in (the weight ratio of Pt to the sample is 3 wt%), and vacuumized under stirring. Pt was in-situ photoreduced onto the catalyst surface under irradiation of a 300-W Xe lamp (CEL-HXF300, Ceaulight, China) for 1 h. Then, the reaction cell was vacuumized again, and the 300-W Xe lamp with a cutoff filter ($\lambda \geq 420$ nm, CEL-UVIRCUT420, Ceaulight) was used as the visible light source for the hydrogen evolution reaction. The amount of generated hydrogen was monitored by gas chromatography (Beifen-Ruili: SP-2100, MS-5 Å column, TCD) with ultrapure Ar as the carrier gas. For measurement of the apparent quantum yield (AQY), a THORLABs FB420-10 band-pass filter ($\lambda$ = 420±2 nm) was substituted for above-mentioned CEL-UVIRCUT420 cutoff filter. Average irradiation intensity ($E$) and the irradiation area ($A$) of the light are 4.0 mW $cm^{-2}$ and 3.46 $cm^2$, respectively. Then, AQY was calculated by the equation, AQY = $(2hcN_A \cdot r_H)/(EA\lambda)\times 100\%$ where $h$, $c$, $N_A$, and $r_H$, are the Planck constant ($6.626\times10^{-34}$ J s), the light rate ($3.0\times10^8$ m $s^{-1}$), the Avogadro's constant ($6.02\times10^{23}$ $mol^{-1}$), and the $H_2$ evolution rate (mol $s^{-1}$), respectively.

Photodegradation reactions were performed on a XPA-7 photocatalytic reaction apparatus (Xujiang Electromechanical Plant, Nanjing, China) at temperature of <35 °C. A 500-W Xe lamp with a cutoff filter ($\lambda \geq 420$ nm) was used as the visible light source. For each run, 0.02 g of the sample was added to 50 mL of 10 mg $L^{-1}$ RhB solution. Then, the suspension was stirred in the dark for 1 h to ensure sorption equilibrium. After light was turned on, ~4 mL of the suspension was taken out and filtered through a 0.45-$\mu$m polyether sulfone membrane at every given time interval. The filtrate was analyzed on a Hewlett-Packard 8453 UV-Vis spectrophotometer (USA) at 554 nm.

***S1.6. Theoretical calculation***

Density functional theory (DFT) calculations corrected by the on-site Coulomb interaction were performed by using the Vienna Ab-initio Simulation package (VASP). [1] The exchange-correlation interaction is described by generalized gradient approximation (GGA) with the Perdew-Burke-Ernzerhof (PBE) functional. [2] To better describe non-bonding interactions, Grimme's scheme van der Waals correction is utilized. [3] The energy cut-off is set to 500 eV. The Brillouin zone is sampled using a Monkhorst-Pack 5 × 5 × 3 $K$-point grid. [4, 5] For all the calculations, spin polarization was taken into account and the convergence criteria for the electronic and ionic relaxation are $10^{-5}$ eV and 0.02 eV/Å, respectively.

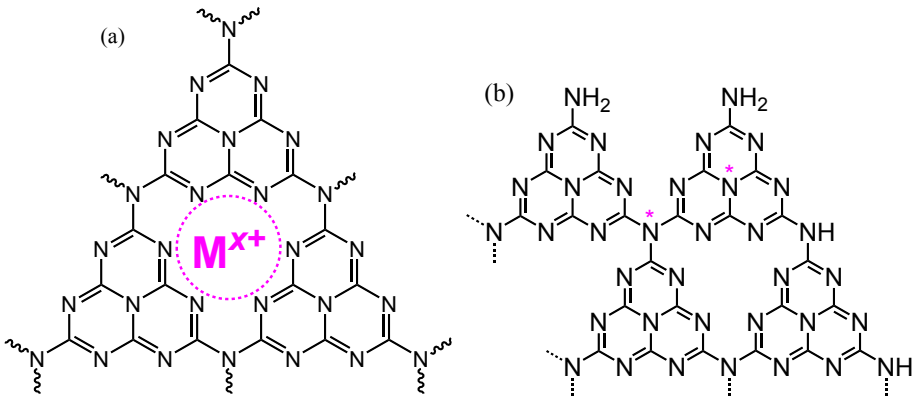


**Fig. S1.** (a) Coordination interactions between doping metal ions with N atoms around the molecular cavity in CN and (b) marking of N-$C_3$ bonds with "*" in framework structure of CN.

**Equation S1.** The probable redox reaction between $(NH_4)_2SnCl_6$ and urea.

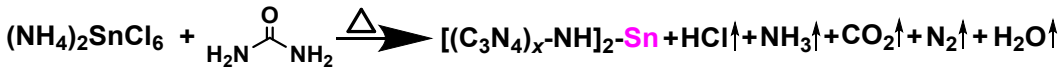


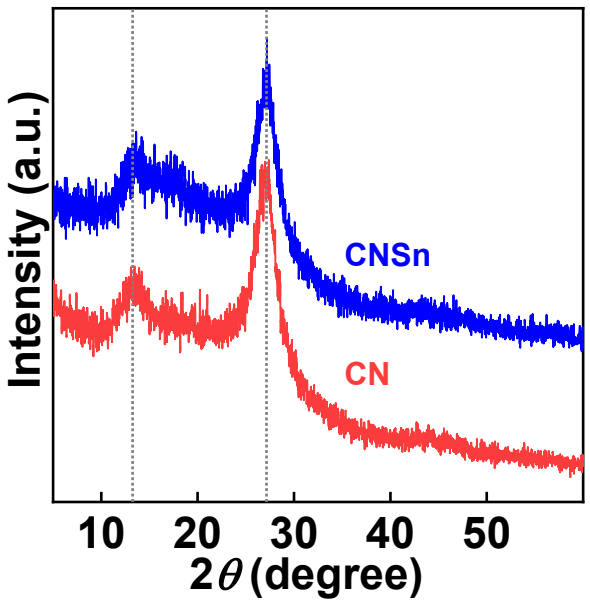


**Fig. S2.** XRD patterns of samples.

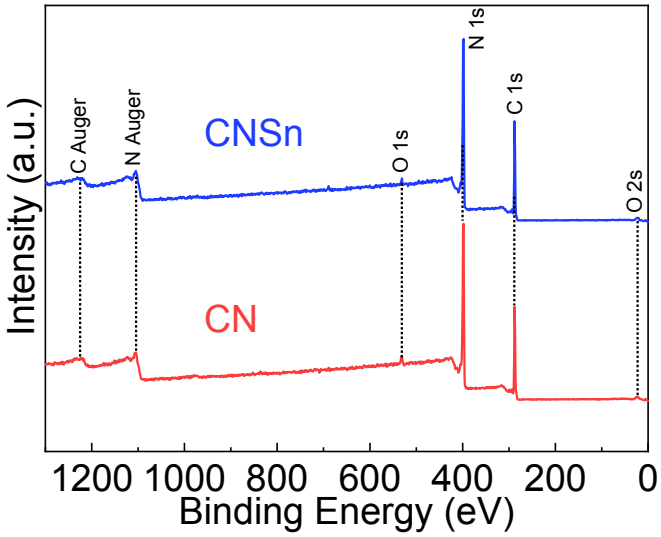


**Fig. S3.** Survey XPS spectra of samples.

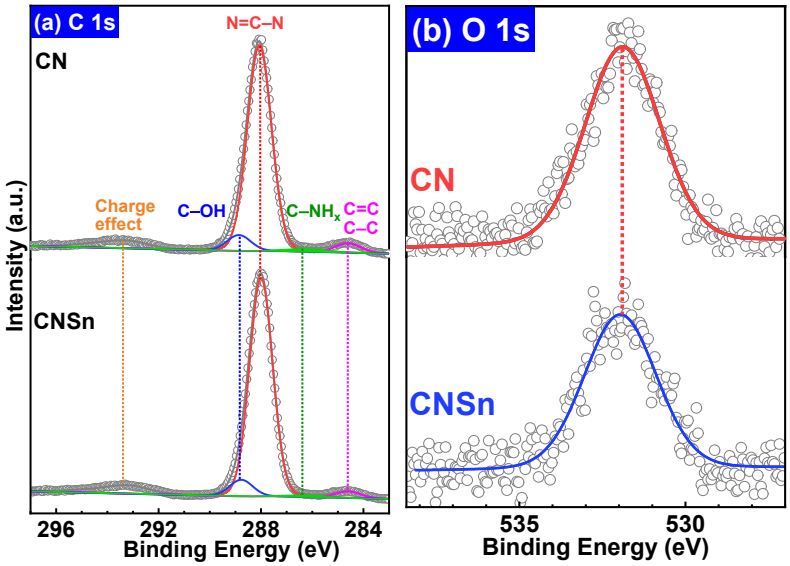


**Fig. S4.** (a) C 1s and (b) O 1s core-level XPS spectra of samples.

In C 1s core-level XPS spectra (Fig. S4a), peaks of CN at ~284.6, 286.4, 288.0, 288.8, and 293.2 eV are assigned to adventitious carbon, C atoms in C–$NH_x$, N=C–N, and surficial C–OH bonds, and charge effect in heterocycles, respectively [6, 7]. In the O 1s core-level spectrum of CN (Fig. S4b), the peak at 531.9 eV is ascribed to surficial adsorbed hydroxyl species [6]. Corresponding peaks of CNSn show similar BE positions as those of CN (ignoring position difference of <0.05 eV).

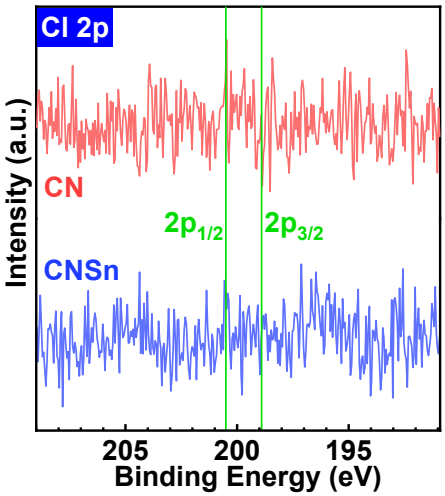


**Fig. S5.** Cl 2p core-level XPS spectra of samples. Two lines in the figure denote theoretical peak positions of Cl $2p_{1/2}$ and $2p_{3/2}$.

**Table S1.** Elemental contents of CN and CNSn calculated from XPS data.

| Sample | N/C molar ratio | Molar content in N (%) | | | $W_{Sn}$ (wt%) |
|---|---|---|---|---|---|
| | | N–H | N–$C_3$ | C=N–C | |
| CN | 1.32 | 7.8 | 23.0 | 69.2 | 0 |
| CNSn | 1.33 | 6.8 | 23.2 | 69.9 | 0.39 |

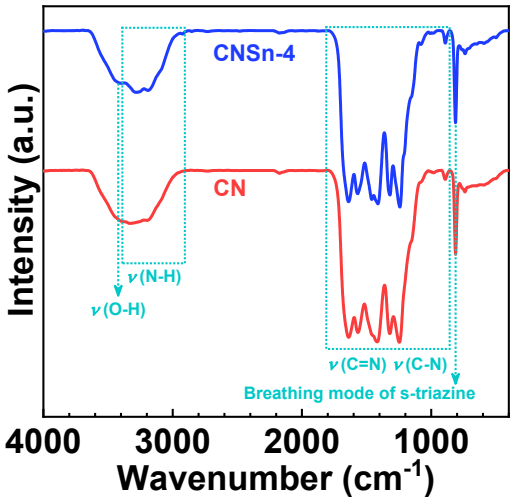


**Fig. S6.** FT-IR spectra of samples.

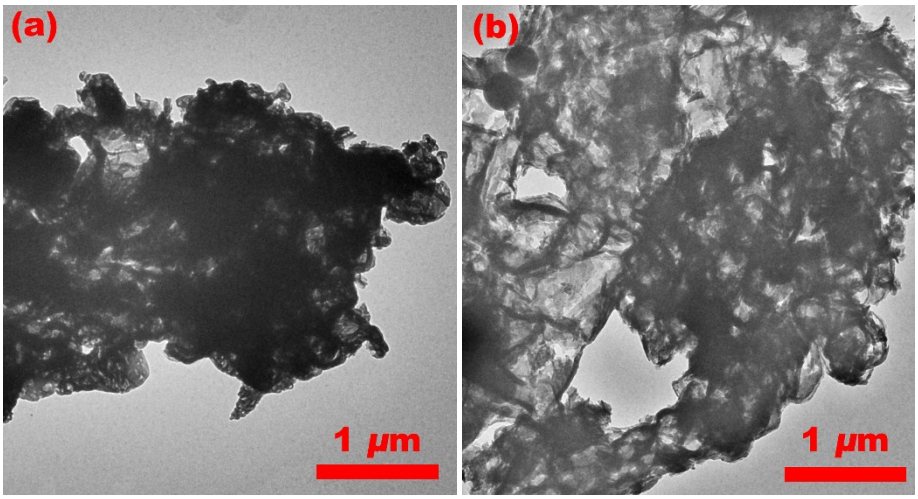


**Fig. S7.** TEM images of (a) CN and (b) CNSn.

As shown in the Fig. S7, the more loose structure of CNSn than that of CN indicates there are more pores in CNSn.

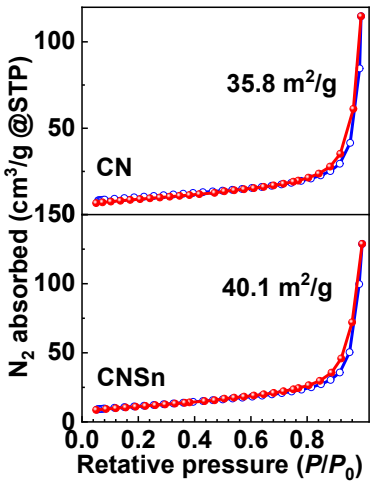


**Fig. S8.** $N_2$ adsorption-desorption isotherms of samples. Number in the figure are BET specific surface areas.

As shown in Fig. S8, all the samples exhibit type-IV isotherms with type-H3 hysteresis loops, indicating existence of slit-like mesopores formed via nanosheet aggregation. [8]

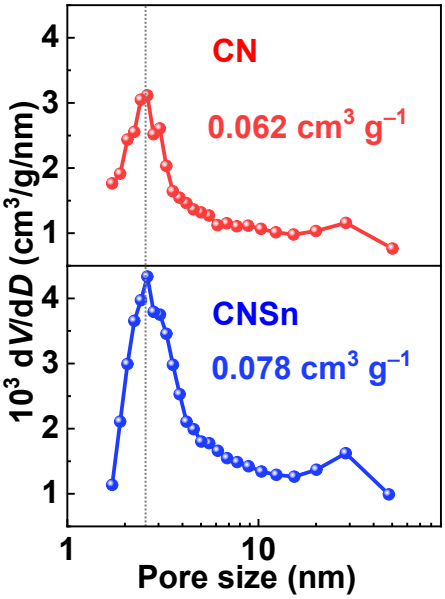


**Fig. S9.** Pore-size distribution curves of samples, calculated from the adsorption branch of isotherms by the BJH method. Numbers in the figure are pore volume.

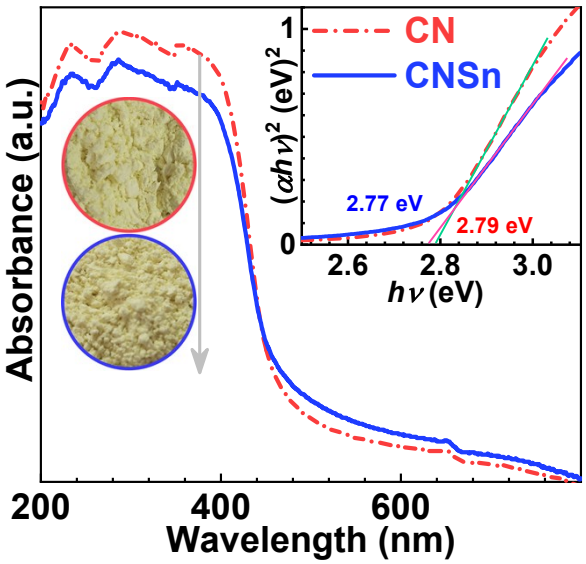


**Fig. S10.** UV-vis diffuse reflectance spectra of samples. The inset is corresponding Tauc plots.

To determine energy bandgaps ($E_g$) of samples, Tauc plots of samples (Inset in Fig. S10) were gained via the equation, $\alpha h\nu = A(h\nu - E_g)^{n/2}$ where $\alpha$, $h$, $\nu$, and $A$ are the absorption coefficient, the Planck constant, the light frequency, and the constant. The parameter $n$ depends on whether the transition of semiconductors is direct ($n$ = 1) or indirect ($n$ = 4). $n$ = 1 was confirmed for CN and CNSn by Parida's method [9]. That is, CN and CNSn are direct bandgap semiconductors [10-12]. Then, $E_g$ values of CN and CNSn were determined to be 2.79 and 2.77 eV, respectively, as shown in the inset.

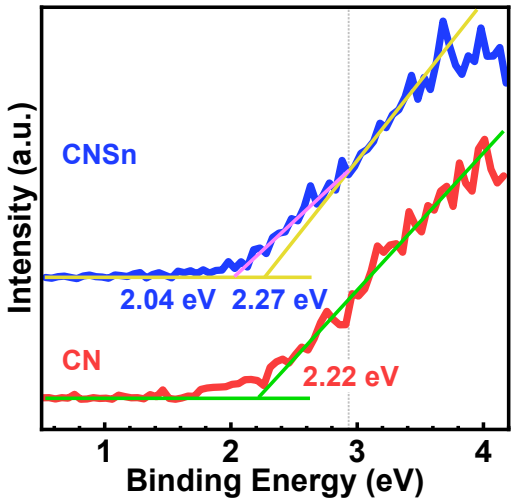


**Fig. S11.** A repeated test on the VB-XPS spectra of samples.

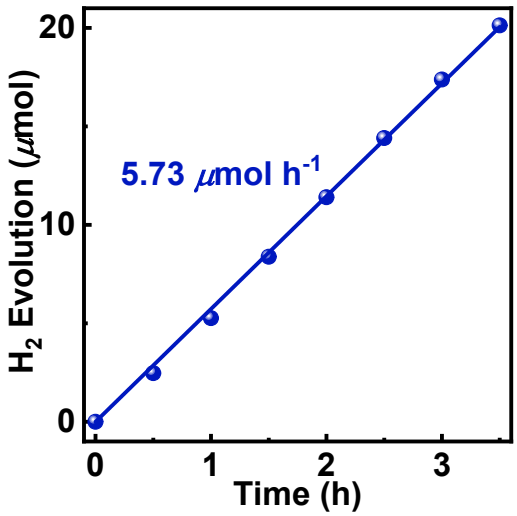


**Fig. S12.** Photocatalytic hydrogen evolution on CNSn under irradiation of 420-nm light.

**Table S2.** Photocatalytic hydrogen evolution rates ($R_H$) and partial experimental conditions for some metal-doped CN.

| Sample | Electron donor | Light source | $R_H$ (mmol $g^{-1}$ $h^{-1}$) | Ref. |
|---|---|---|---|---|
| **CNSn** | Triethanolamine (10 vol%) | 300 W Xe lamp ($\lambda$> 420 nm) | **1.69** | **This work** |
| K-doped CN | Triethanolamine (10 vol%) | 300 W Xe lamp (2500 > $\lambda$ > 420 nm) | 1.0 | [13] |
| Co-doped CN | Triethanolamine (20 vol%) | 300 W Xe lamp | 0.2 | [14] |
| Pt-doped CN | Triethanolamine (10 vol%) | 300 W Xe lamp ($\lambda$ > 400 nm) | 0.6 | [15] |
| Zn-doped CN | Methanol (18.5 vol%) | 200 W Xe lamp ($\lambda$ > 420 nm) | 0.3 | [16] |
| Na-doped CN | Triethanolamine (10 vol%) | 300 W Xe lamp ($\lambda$> 420 nm) | 0.2 | [17] |
| Li-doped CN | Triethanolamine (10 vol%) | 350 W Xe lamp ($\lambda$> 400 nm) | 0.2 | [18] |
| …… | …… | …… | …… | …… |

**Table S3.** Fitting results of data in Fig. 4b to a pseudo-first-order kinetics model ($\ln(C/C_0) = -kt$, where $k$ is the rate constant).

| Sample | $k$/$h^{-1}$ | Adj. $R^2$ |
|---|---|---|
| CN | 2.10 | 0.9927 |
| CNSn | 7.38 | 0.9951 |

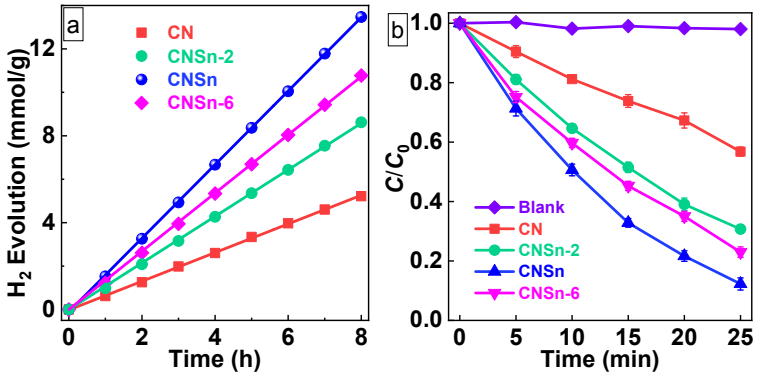


**Fig. S13.** (a) Photocatalytic hydrogen evolution and (b) RhB photodegradation on various samples under visible light irradiation. Apparently, CNSn exhibits the highest photoactivity for both PHE and RhB degradation.

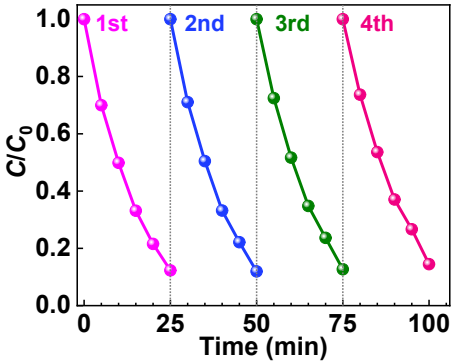


**Fig. S14.** Cyclic experiments of RhB photodegradation on CNSn.

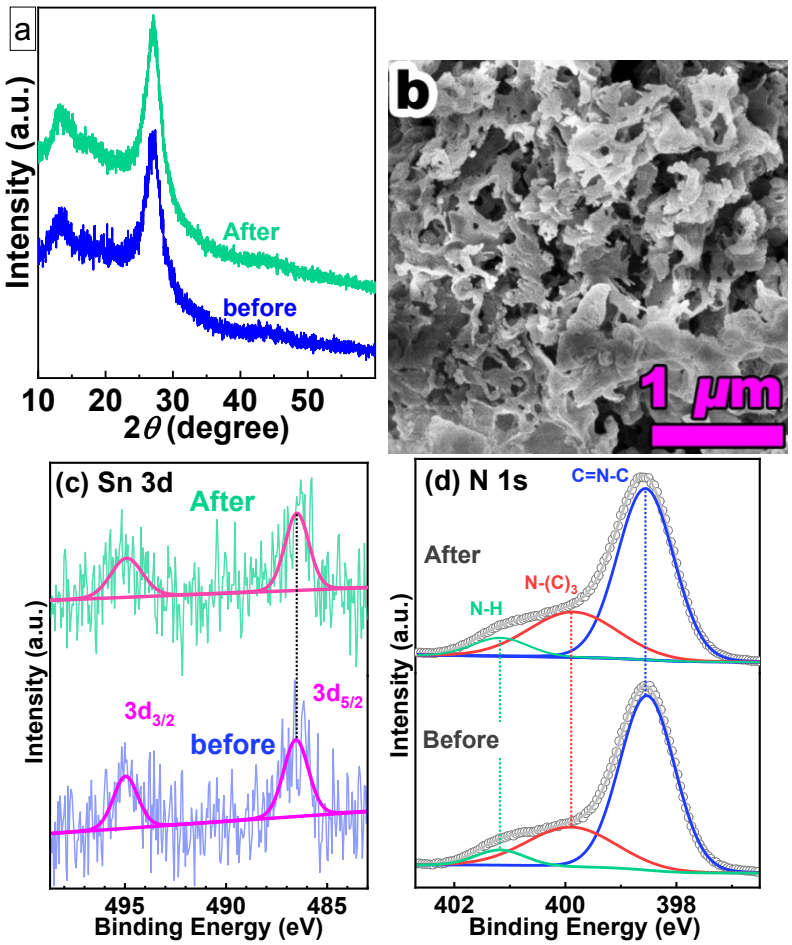


**Fig. S15.** (a) XRD patterns of CNSn before and after the cyclic experiments; (b) the SEM image of CNSn after the cyclic experiments; and (c) Sn 3d and (d) N 1s XPS core-level spectra of CNSn before and after the cyclic experiments.

**References**

1 G. Kresse and J. Furthmüller, *Phys. Rev. B*, 1996, **54**, 11169.

2 J. P. Perdew, K. Burke and M. Ernzerhof, *Phys. Rev. Lett.*, 1996, **77**, 3865.

3 S. Grimme, J. Antony, S. Ehrlich and H. Krieg, *J. Chem. Phys.*, 2010, **132**, 154104.

4 Y. Zheng, L. Lin, B. Wang and X. Wang, *Angew. Chem. Int. Ed.*, 2015, **54**, 12868.

5 T. Xiong, W. Cen, Y. Zhang and F. Dong, *ACS Catal.*, 2016, **6**, 2462.

6 H. Li, J. Liu, W. Hou, N. Du, R. Zhang and X. Tao, *Appl. Catal. B*, 2014, **160-161**, 89.
7 S. Yu, J. Li, Y. Zhang, M. Li, F. Dong, T. Zhang and H. Huang, *Nano Energy*, 2018, **50**, 383.
8 S. Liu, J. Chen, D. Xu, X. Zhang and M. Shen, *J. Mater. Res.*, 2018, **33**, 1391.
9 L. Mohapatra, K. Parida and M. Satpathy, *J. Phys. Chem. C*, 2012, **116**, 13063.
10 Y. Liu, Y.-X. Yu and W.-D. Zhang, *Int. J. Hydrogen Energy*, 2014, **39**, 9105.
11 X. Yang, F. Qian, Y. Wang, M. Li, J. Lu, Y. Li and M. Bao, *Appl. Catal. B*, 2017, **200**, 283.
12 P. Niu, L. Zhang, G. Liu and H.-M. Cheng, *Adv. Funct. Mater.*, 2012, **22**, 4763.
13 M. Wu, J. M. Yan, X. N. Tang, M. Zhao and Q. Jiang, *ChemSusChem*, 2014, **7**, 2654.
14 Y. Cao, S. Chen, Q. Luo, H. Yan, Y. Lin, W. Liu, L. Cao, J. Lu, J. Yang, T. Yao and S. Wei, *Angew. Chem. Int. Ed.*, 2017, **56**, 12191.
15 Y. Li, Z. Wang, T. Xia, H. Ju, K. Zhang, R. Long, Q. Xu, C. Wang, L. Song, J. Zhu, J. Jiang and Y. Xiong, *Adv. Mater.*, 2016, **28**, 6959.
16 B. Yue, Q. Li, H. Iwai, T. Kako and J. Ye, *Sci. Technol. Adv. Mater.*, 2011, **12**, 034401.
17 Y. Shang, Y. Ma, X. Chen, X. Xiong and J. Pan, *Mol. Catal.*, 2017, **433**, 128.
18 J. Jiang, S. Cao, C. Hu and C. Chen, *Chin. J. Catal.*, 2017, **38**, 1981.